European Journal of Chemistry

Preparation of novel compounds, characterization and studying experimentally and theoretically as inhibitors through thermodynamic and quantum chemistry

Mushtaq Jerri Meften

Education Directorate of Basrah, Ministry of Education, Basrah, 61001, Iraq

* Corresponding author at: Education Directorate of Basrah, Ministry of Education, Basrah, 61001, Iraq.
Tel.: +964.40.7705639149. Fax: +964.40.7705639149. E-mail address: mushtak9791@yahoo.ca (M.J. Meften).

ARTICLE INFORMATION

ABSTRACT

To inhibit corrosion of the mild steel Q235 type in cooling water systems, two heterocyclic compounds were used, namely (3-(2-hydroxy-3-methoxyphenyl)-5-(4-nitrophenyl)-2-(4-((4-nitrophenyl)diazennyl)phenyl)dihydro-*2H*-pyrrolo[3,4-*d*]isoxazole-4,6(5*H*,6a*H*)-dione) (A1), and (5-(4-(1,3,5-dithiazinan-5-yl)phenyl)-5-pentyl-1,3,5-dithiazinan-5-ium (A2). They were experimentally evaluated by weight loss method at deference concentrations from 1×10^{-1} M to 1×10^{-5} M at 5 hours, and theoretically through thermodynamic functions, such as activation energy, standard free energy of adsorption, enthalpy of adsorption and entropy of adsorption. On the other hand, they were theoretically studied through quantum chemistry, such as quantum parameters including Highest occupied molecular orbital (HOMO) energy, Lowest unoccupied molecular orbital (LUMO) energy, energy gap, dipole moment, chemical potential, $\Delta E_{Back-donation}$, global hardness, global softness, global electrophilicity index, ionization potential, electro negativity and number of transferred electrons. The temperature effect on the corrosion rate has been studied at 25, 35, 45, 55 and 65 °C, and the adsorption for studied inhibitors on mild steel surface obeyed Langmuir adsorption isotherm. The methods of compounds preparation A1 and A2 are different from each other, A1 was prepared through several steps, and A2 through the domino reaction (by two step). The results indicate that the studied inhibitors exhibit good performance as an inhibitors for mild steel corrosion in cooling water systems, and inhibition efficiency increasing with increase inhibitors concentration and decreased with temperature rise.

1. Introduction

Corrosion is the degradation of materials properties through the reaction chemical or electrochemical with its environment. Theoretical chemistry has been used recently to explain the mechanism of corrosion inhibition, such as quantum chemical calculations [1,2]. Inhibition of corrosion by using organic inhibitors mostly depends on adsorption of inhibitor molecules on the metal surface, thus the formation of a protective film on metal surface minimizes access of corrosive ions to it. Generally, selection of these organic inhibitors have been based on an empirical approach, many attempts have been made to correlate inhibition efficiency with properties of organic molecules (inhibitors) such as, geometrical dimension, π-bonding, electron pairs in hetero atoms, metal ionization potential, steric effects and molecular structure [3-5]. Heterocyclic compounds containing nitrogen and oxygen atoms are good corrosion inhibitors for many metals and alloys in various aggressive media [6]. The structure of compounds and the electronic parameters that can be obtained through theoretical calculations of quantum chemistry such as HOMO energy, LUMO energy and the energy gap ($\Delta E = E_{LUMO} - E_{HOMO}$) have been found to be quite useful to investigate the reaction mechanisms of inhibitor molecules and its electronic states [7-10]. The thermodynamic functions have been calculated to explain the adsorption process on the metal surface and its discussion [11]. Temperature has a great effect on the rate electrochemical corrosion. The increase in temperature on neutral corrosion solutions has a favourable effect on the potential of oxygen depolarization and its diffusion [12]. Kinetic and thermodynamic parameters are useful tools for clarifying the adsorption behaviour of an inhibitor on the metal surface, thus they explain the adsorption process [13,14], if the $\Delta H_{ads} > 0$ (endothermic process) this means chemisorptions, if the negative heat of adsorption $\Delta H_{ads} < 0$ (exothermic process) may involve either physisorption, chemisorptions or mixture of both [15]. Due to the continued interest for using inhibitors to reduce metals corrosion this study has been aimed to prepared new heterocyclic compounds and their experimentally investigation as an inhibitors through weight loss method and also theoretically investigated through thermodynamic and quantum chemistry.

2. Experimental

2.1. Materials

Corrosion tests were performed on a freshly specimens of mild steel Q235 type and equipped from company Hebei Jimeng Yongxing Flange Pipe Fittings Co., Ltd, China. Its chemical composition is 0.16 %C, 0.53 %Mn, 0.30 %Si, 0.025 %P, 0.015% S and 98.97 %Fe [16]. Used specimens in weight loss experiments have been cut mechanically to 6.0×4.0×0.5 cm for length, width and thickness respectively, so its area is 58 cm². Cooling water systems have been equipped from the petrochemical plant, and all chemical materials were procured from Sigma-Aldrich, Merck and BDH companies.

2.2. Corrosion measurements

Mild steel specimens have been polished by using a series of silicon carbide papers SiC (120, 320, 800 grit size) then rinsed in distilled water, acetone and dried in a desiccators to be used in weight loss experiments. After weighing the specimens accurately in digital balance they have been immersed in cooling water as a corrosive medium for 5 hours in absence and presence of inhibitors **A1** and **A2** at different concentrations and temperatures. Then, the specimens were taken out of a corrosive medium and washed by distilled water in order to remove products of corrosion. After that they were dried in a desiccator and weighed again. The difference in weight before and after immersion represents weight loss

2.3. Synthesis and characterization of 3-(2-hydroxy-3-methoxyphenyl)-5-(4-nitrophenyl)-2-(4-((4-nitrophenyl) diazennyl)phenyl)dihydro-2H-pyrrolo[3,4-d] isoxazole-4,6(5H,6aH)-dione (A1)

Step 1: Synthesis of phenyl hydroxyl amine: Nitro benzene (6.6 mL) has been added to 4 g of ammonium chloride and 128 mL water, the mixture was stirred in beaker at 50-60 °C. Then, 9.4 g of zinc powder was added to the mixture for 15 min then left for 30 min. After that it has been filtered and saturated by using sodium chloride. It was extracted by using chloroform and the organic layer precipitated by using a hexane and kept it in a dark cool place (109 g/mol).

Step 2: Synthesis of *N*-(2-hydroxy-3-methoxybenzylidene) aniline oxide: 2-Hydroxy-3-methoxybenzeldehyde (0.76 g; 0.005 mol) and phenyl hydroxyl amine (0.545 g; 0.005 mol) prepared in Step 1 have been dissolved in 100 mL of absolute ethanol for 2 hours within refluxing. The precipitate has been formed and cooled, then it was filtered to produce *N*-(2-hydroxy-3-methoxybenzyldene)aniline oxide.

Step 3: Synthesis of 1-(4-nitrophenyl)-1*H*-pyrrole-2,5-dione: A mixture consists of *p*-nitro aniline (1.38 g; 0.01 mol) and of maleic anhydride (0.98 g; 0.01 mol) have been stirred for about 2 hours in 50 mL ethanol, then it was filtered to produce precipitate (precipitate of intermediate state). Acetic anhydride (10.5 mL) and sodium acetate (1.09 g) have been added to 4.94 g of formed precipitate (precipitate of intermediate state) and was stirred for about 1.5 hours in water bath at 90 °C, then it was cooled for room temperature to produce 1-(4-nitrophenyl)-1*H*-pyrrole-2,5-dione.

Step 4: Synthesis of heterocyclic compound: *N*-(2-hydroxy-3-methoxybenzylidene)aniline oxide (1.215 g; 0.005 mol) prepared in Step 2 and 1-(4-nitrophenyl)-1*H*-pyrrole-2,5-dione (0.935 g; 0.005 mol) prepared in Step 3 have been blending at a refluxing in 150 mL chloroform for 5 hours, then this mixture was cooled and precipitated by using hexane, and finally it was filtered to produce 3-(2-hydroxy-3-methoxy phenyl)-5-(4-nitrophenyl)-2-phenyldihydro-2*H*-pyrrolo[3,4-*d*]isoxazole-4,6(5*H*,6aH)- dione.

Step 5: Synthesis of diazonium salt: *p*-Nitro aniline (0.138 g; 0.001 mol) in 0.5 mL HCl with 20 mL water at 3 °C has been dissolved (**I**). Sodium nitrite (0.08 g) in 10 mL water at 3 °C has been dissolved (**II**). The solutions **I** and **II** were blending at 3 °C to produce diazonium salt.

Step 6: Synthesis of final compound (Isoxazolidine): Finally, 0.461 g of heterocyclic compound prepared in Step 4 has been blending with diazonium salt prepared in Step 5 in stirred at 3 °C, and neutralized by using hydrochloric acid, then left for 24 hours at 3 °C, after that the mixture was filtered to produce 3-(2-hydroxy-3-methoxyphenyl)-5-(4-nitrophenyl)-2-(4-((4-nitrophenyl)diazennyl)phenyl)dihydro-2*H*-pyrrolo[3,4-*d*]isoxazole-4,6(5*H*,6aH)-dione (**A1**). Scheme 1 illustrates synthesis mechanism of compound **A1**. Color: Brown. Yield: 45%. M.p.: 211-213 °C. FT-IR (KBr, ν, cm^{-1}): 3321 (br, OH), 3070 (CH-aromatic), 2982 (CH-aliphatic), 1703 (C=O), 1600 (C=C), 1188 (C-O), 1452 (N=N), 1396, 1429 (CH-bending), 1097 (C-N). ^{1}H NMR (500 MHz, CDCl₃, δ, ppm): 1.691 (s, 3H, CH₃), 2.390-2.488 (d, 1H, N-CH), 3.331-3.450 (d, 1H, O-CH), 4.291-4.700 (m, 1H, CH-C*H*-C=O), 6.11 (br, s, 1H, OH), 7.491-8.089 (m, 15H, Ar-H), 7.12 (s, CDCl₃) (Figures 1 and 2) [17-19].

2.4. Synthesis and characterization of 5-(4-(1,3,5-dithiazin an-5-yl)phenyl)-5-pentyl-1,3,5-dithiazinan-5-ium (A2)

This compound was prepared in one pot through domino reaction. One pot contains mixture (4.86 mL, 60 mmol) of aqueous solution 37% formaldehyde, 100 mL methanol and (1.08 g; 10 mmol) of 1,4-diamino benzene, which stirred at room temperature for 2 hours, then 40 mmol H₂S gas was added to the mixture for 1 hour and filtered to produce white precipitate. After that 10 mmol of 1-chloropentane and 100 mL of absolute ethanol have been added to the whole mixture at a refluxing for 5 hours to produce 5-(4-(1,3,5-dithiazinan-5-yl)phenyl)-5-pentyl-1,3,5-dithiazinan-5-ium (**A2**). Scheme 2 illustrates synthesis mechanism of compound **A2**. Color: White. Yield: 63%. M.p.: 165-167 °C. FT-IR (KBr, ν, cm^{-1}): 3041 (CH-aromatic), 2960 (CH-aliphatic), 1109 (C-N), 1597 (C=C), 680 (br, C-S), 1407 (CH-bending). ^{1}H NMR (500 MHz, CDCl₃, δ, ppm): 0.921-1.031 (t, 3H, CH₃), 1.211-1.410 (m, 2H, CH₃-C*H₂*), 2.144-2.291 (t, 4H, CH₃-CH₂-C*H₂*-C*H₂*), 2.821-2.911 (t, 2H, N⁺-C*H₂*-CH₂), 3.521 (s, 4H, N⁺-CH₂-S), 4.375 (s, 4H, N-CH₂-S), 5.481 (br, s, 4H, S-CH₂-S), 7.200 (s, CDCl₃), 7.600-7.811 (m, 4H, Ar-H) (Figures 3 and 4) [17-19].

3. Results and discussion

3.1. Effect of inhibitors concentration

In experiments of weight loss, mild steel coupons have been completely immersed in 200 mL of cooling water in open beaker, size 250 mL, for 5 hours in absence and presence compounds at different concentrations. The beaker has been inserted into a water bath for keeping the temperature at 298 K. From the weight loss results obtained, inhibition efficiency *% IE*, corrosion rate *CR* and degree of surface coverage *θ* have been calculated by using Equations 1, 2 and 3, respectively [20].

$$IE\% = \frac{W_{blank} - W_{inhibitor}}{W_{blank}} \times 100 \qquad (1)$$

$$CR = \frac{\text{Weight loss of mild steel (g)}}{\text{Surface area of mild steel (cm}^2) \times \text{Time (h)}} \qquad (2)$$

$$\text{Surface conerage} = \frac{W_{blank} - W_{inhibitor}}{W_{blank}} \qquad (3)$$

where W_{blank} and $W_{inhibitor}$ are the weight loss of mild steel in absence and presence of inhibitors respectively, and θ is the degree of metal surface coverage by inhibitors. From the results shown in Table 1, the decrease of both weight loss and corrosion rate with concentration increase can be observed. Figures 5 and 6 have been shown decrease of corrosion rate and increase efficiency of inhibition with increasing concentration of compounds **A1** and **A2**.
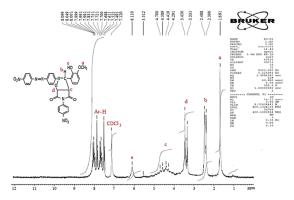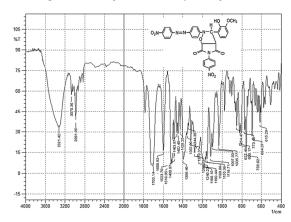
Figure 1. ^{1}H NMR spectrum of heterocyclic compound **A1**.

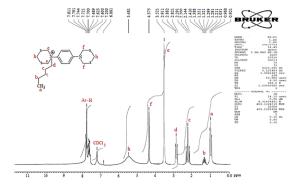**Figure 2.** FT-IR spectrum of heterocyclic compound **A1**.

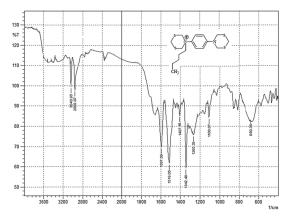**Figure 3.** ^{1}H NMR spectrum of heterocyclic compound **A2**

Figure 4. FT-IR spectrum of heterocyclic compound **A2**.

Scheme 1

The reason is due to the increased amount of the used inhibitor, thereby increasing the metal surface area which covered by molecules of inhibitor; therefore, the adsorption process increases and prevents the arrival of corrosive material to surface, and finally increases the efficiency of inhibition. Also, perhaps the reason is due to the numerous presence from action centers in the structures of compound **A1** and **A2** such as double bonds, π-bonds and electron pairs of atoms N, S and O, therefore are likely to π-electrons and non-bonding electrons in hetero atoms can provide suitable places for direct absorption on metal surface which based on of donor acceptor interactions between π-electrons with non-bonding electrons and vacant *d*-orbitals of mild steel atoms, hence adsorption process facilitated and inhibition efficiency

increased [21-24]. The values of inhibition efficiency and corrosion rate obtained at different concentrations indicated to decrease clearly in the corrosion processes of mild steel in presence of inhibitors, thus the inhibition efficiency increases to reach the higher value 94.98% of compound **A1** and 91.64% of compound **A2** at 1×10^{-1} M.

3.2. Thermodynamic functions and temperature effect

Study temperature effect on the metals corrosion is very complex because many of changes occur on the metal surface such as, rapid etching, desorption of inhibitor and the inhibitor itself may undergo decomposition.

Table 1. Corrosion parameters of mild steel in cooling water at deferent concentrations of compounds **A1** and **A2** at 298 K for 5 hours.

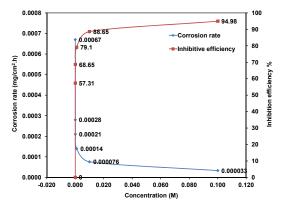| Inhibitors	Concentration (M)	Weight (g)	Corrosion rate (CR) (mg/cm² h)	Inhibition efficiency (%)	θ
Blank	0.00	0.1954	6.7×10^{-4}	-	-
A1	1×10^{-5}	0.0834	2.8×10^{-4}	57.31	0.5731
	1×10^{-4}	0.0618	2.1×10^{-4}	68.65	0.6865
	1×10^{-3}	0.0421	1.4×10^{-4}	79.10	0.7910
	1×10^{-2}	0.0221	7.6×10^{-5}	88.65	0.8865
	1×10^{-1}	0.0098	3.3×10^{-5}	94.98	0.9498
A2	1×10^{-5}	0.0804	2.7×10^{-4}	59.70	0.5970
	1×10^{-4}	0.0628	2.1×10^{-4}	68.65	0.6865
	1×10^{-3}	0.0441	1.5×10^{-4}	77.61	0.7761
	1×10^{-2}	0.0242	8.3×10^{-5}	87.61	0.8761
	1×10^{-1}	0.0165	5.6×10^{-5}	91.64	0.9164

Scheme 2

Figure 5. Variation of corrosion rate and inhibition efficiency against the different concentrations of compound **A1** at 298 K.

Temperature is an important kinetic factor and it influences the corrosion rate of metals and reduces inhibitors adsorption on surface of metals. In order to study the effect of temperature and elucidate that on the corrosion rate and efficiency of inhibition, the experiments have been conducted in 298, 308, 318, 328 and 338 K with and without inhibitors for 5 hours. Results in Tables 2 and 3, and Figure 7 have been

shown that the temperature has a great effect on corrosion rate that increases with temperature rises with and without inhibitors. Besides, the raise of temperature leads to a decrease of inhibition efficiency and the reason is probably increasing the kinetic energy of inhibitor molecules and move away from the metal surface, and finally this leads to an increase in rate of corrosion and decrease of efficiency. Also, decrease of inhibition efficiency perhaps back to weakening of physical adsorption which occurs on the metal surface, or may be due to increased rate of desorption inhibitor from the mild steel surface gradually at high temperatures. All results have been shown decreases of inhibition efficiency with temperature raise [25-30].

The corrosion inhibition of mild steel by using prepared compounds could be well explained through thermodynamic functions, the enthalpy of adsorption $\Delta H°$, standard free energy of adsorption $\Delta G°$ and entropy of adsorption $\Delta S°$. These functions have been calculated to elucidate the inhibitors action in inhibition process and that is through transition state Equation 4, also activation energy E_a of the corrosion process of mild steel has been calculated by using Equation 5 [31].

$$CR = \frac{RT}{Nh} \exp\left(\frac{\Delta S°}{R}\right) \exp\left(\frac{-\Delta H°}{RT}\right) \qquad (4)$$

$$\text{Ln} \frac{r_2}{r_1} = \frac{\{Ea(T_2 - T_1)\}}{R(T_2 \times T_1)} \qquad (5)$$

Table 2. Corrosion rate of mild steel in cooling water with presence of inhibitor **A1**.

Corrosion rate (mg/cm² h) of compound A1 at different temperatures					
Concentration (M)	298 K	308 K	318 K	328 K	338 K
0.00	6.7×10^{-4}	7.9×10^{-4}	9.9×10^{-4}	1.9×10^{-3}	3.3×10^{-3}
1×10^{-5}	2.8×10^{-4}	4.3×10^{-4}	6.4×10^{-4}	8.4×10^{-4}	9.9×10^{-4}
1×10^{-4}	2.1×10^{-4}	3.1×10^{-4}	4.2×10^{-4}	6.2×10^{-4}	8.1×10^{-4}
1×10^{-3}	$1.4 \times 10_{-4}$	2.6×10^{-4}	3.2×10^{-4}	5.4×10^{-4}	6.8×10^{-4}
1×10^{-2}	7.6×10^{-5}	9.1×10^{-5}	9.8×10^{-5}	4.2×10^{-4}	5.5×10^{-4}
1×10^{-1}	3.3×10^{-5}	5.2×10^{-5}	7.1×10^{-5}	2.1×10^{-4}	3.2×10^{-4}

Table 3. Corrosion rate of mild steel in cooling water with presence of inhibitor **A2**.

Corrosion rate (mg/cm² h) of compound A2 at different temperatures					
Concentration (M)	298 K	308 K	318 K	328 K	338 K
0.00	6.7×10^{-4}	7.9×10^{-4}	9.9×10^{-4}	1.9×10^{-3}	3.3×10^{-3}
1×10^{-5}	2.7×10^{-4}	5.1×10^{-4}	6.3×10^{-4}	7.9×10^{-4}	9.2×10^{-4}
1×10^{-4}	2.1×10^{-4}	4.8×10^{-4}	5.7×10^{-4}	6.6×10^{-4}	7.9×10^{-4}
1×10^{-3}	1.5×10^{-4}	3.7×10^{-4}	4.5×10^{-4}	5.8×10^{-4}	6.2×10^{-4}
1×10^{-2}	8.3×10^{-5}	9.7×10^{-5}	2.9×10^{-4}	3.8×10^{-4}	4.4×10^{-4}
1×10^{-1}	5.7×10^{-5}	7.7×10^{-5}	2.1×10^{-4}	3.0×10^{-4}	3.9×10^{-4}

where CR is the corrosion rate, R is the gases constant 8.314 J/mol.K, T_1 and T_2 are the absolute temperatures, h is the Plank's constant 6.626176×10^{-34} J.s and N is Avogadro's number 6.02252×10^{23} 1/mol. E_a is the activation energy for corrosion process, $\Delta H°$ is the enthalpy of adsorption, $\Delta S°$ is the entropy of adsorption. r_1 and r_2 are corrosion rate at deferent temperatures [24,32,33]. The $\Delta G°$ has been calculated by using Equation of Gibbs-Helmholtz (6) depending on $\Delta H°$ and $\Delta S°$ functions [34-36].

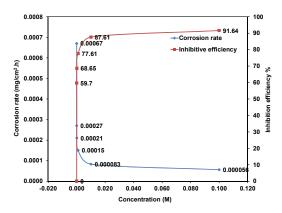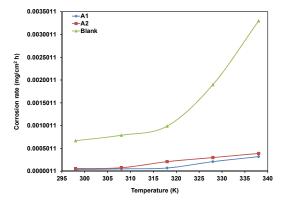$$\Delta G° = \Delta H° - T\Delta S° \tag{6}$$

Figure 6. Variation of corrosion rate and inhibition efficiency against the different concentrations of compound **A2** at 298 K.

Figure 7. Variation of corrosion rate of mild steel in cooling water at optimum concentration 1×10^{-1} M of compounds **A1** and **A2** at different temperatures.

On the light of plots of log (CR/T) versus 1/T, the straight lines have been obtained as shown in Figures 8 and 9. From slope and intercept the $\Delta H°$ and $\Delta S°$ have been calculated as shown in Equations 7 and 8, respectively [25,37,38].

$$\text{Slope} = \frac{-\Delta H°}{2.303 \times R} \tag{7}$$

$$\text{Intercept} = \log\left(\frac{R}{Nh}\right) + \frac{\Delta S°}{2.303 \times R} \tag{8}$$

It is clear from results shown in the Table 4 and Figures 8 and 9, the entropy in the inhibitor presence **A1** at concentrations 1×10^{-1} M and 1×10^{-2} M has been increased in comparison with the blank sample that indicates the increased disorderliness in going from reactant to compounds activation, whereas in other concentrations the decrease of entropy (large negative values) have been noted, this means that in the rate determining step represented that there is an association rather than dissociation. In some concentrations the values of entropy remains almost constant (slight change) in comparison with blank. The values of $\Delta S°$ are negative for both the inhibited and uninhibited systems, this might interpret inhibitors adsorption on mild steel surface through quasi-substitution process between the heterocyclic compounds in the aqueous phase [Org.(*in aqueous*)] and water molecules on mild steel surface [H₂O(*ads*)] as shown Equation 9 [25,35,39-41].

$$\text{Org. molecules}_{(aq)} + x\text{H}_2\text{O}_{(ads.)} \rightarrow \text{Org. molecules}_{(ads.)} + x\text{H}_2\text{O}_{(aq)} \tag{9}$$

The positive values of enthalpy $\Delta H°$ means the dissolution process of mild steel which is endothermic suggesting that the dissolution of mild steel in presence of inhibitors are slow, also it means that adsorption which occurred on the mild steel surface is chemical adsorption. The $\Delta H°$ values in inhibitors presence are lower mostly than that in its absence, this due to the decrease of the energy barrier of corrosion reaction occurring on the mild steel surface [42-44]. The activation energy values E_a in presence of inhibitors are greater than its absence, this indicates that the corrosion reaction of mild steel has been inhibited by using compounds **A1** and **A2**. The increase of activation energies values signify that the adsorption which has been occurred is physical adsorption. The change in values of E_a at inhibitors presence is not at the same pace due to the modification of mechanism of corrosion process and its decrease [38,45,46]. The $\Delta G°$ values listed in Table 4 are positive and increase with increasing both of concentration and temperature. This indicates that the compounds **A1** and **A2** are stable inhibitors on the surface of mild steel [34,38].

Table 4. Thermodynamic functions of mild steel dissolution in cooling water in absence and presence of compounds **A1** and **A2** at deferent concentrations and temperatures.

Inhibitor concentration (M)	Temperature (K)	Compound A1				Compound A2			
		E_a (kJ/mol)	$\Delta G°$ (kJ/mol)	$\Delta H°$ (kJ/mol)	$\Delta S°$ (J/mol·K)	E_a (kJ/mol)	$\Delta G°$ (kJ/mol)	$\Delta H°$ (kJ/mol)	$\Delta S°$ (J/mol.K)
0.00 (Blank)		12.51	91.19	31.30	-201.56	12.51	91.19	31.30	-201.56
1×10⁻⁵	298	32.66	92.91	24.08	-231.26	48.45	92.52	21.30	-239.82
	308		95.22				94.91		
	318		97.53				97.30		
	328		99.84				99.69		
	338		102.15				102.08		
1×10⁻⁴	298	29.68	93.67	25.73	-228.64	63.03	93.07	22.75	-236.72
	308		95.95				95.43		
	318		98.23				97.79		
	328		100.51				100.15		
	338		102.79				102.51		
1×10⁻³	298	47.23	94.49	30.13	-216.74	68.67	94.04	25.50	-230.04
	308		96.65				96.34		
	318		98.81				98.64		
	328		100.97				100.94		
	338		103.13				103.24		
1×10⁻²	298	13.73	96.50	41.08	-186.17	11.82	95.64	31.57	-215.08
	308		98.36				97.79		
	318		100.22				99.94		
	328		102.08				102.09		
	338		103.94				104.24		
1×10⁻¹	298	34.64	98.51	46.96	-173.72	22.89	96.63	37.03	-200.96
	308		100.24				98.63		
	318		101.97				100.63		
	328		103.70				102.63		
	338		105.43				104.63		

Table 5. Shows the adsorption parameters of inhibitors **A1** and **A2** in cooling water at 298 K.

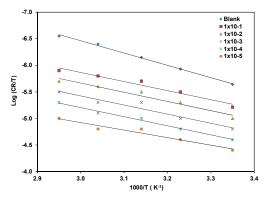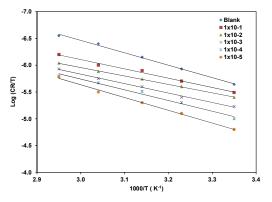| Inhibitors	Adsorption isotherm	r^2	Slope	Intercept	K_{ads}	$\Delta G°$ (kJ/mol)
A1	Langmuir	0.999990	1.04848	0.000185	5405.40	-31.245
A2	Langmuir	0.999991	1.08855	0.000179	5586.59	-31.327

Figure 8. Transition state plots for corrosion rates of mild steel in cooling water with presence of compound **A1** at different concentrations.

Figure 9. Transition state plots for corrosion rates of mild steel in cooling water with presence of compound **A2** at different concentrations.

3.3. Behaviour of adsorption isotherm

It is essential to know the mode of adsorption inhibitors because the adsorption isotherms provide valuable basic information on the interaction between the inhibitors and metal surface, and the adsorption mechanism depends on the electronic characteristics of the inhibitor, the nature of metal surface and temperature. The experimental data has been applied on various adsorption isotherms and the Langmuir adsorption isotherm has been found to be the best description of inhibitors studied through the relationship between concentration versus (concentration/θ) which has been calculated by using Equation 10 [32,45,47].

$$\frac{C_{inh}}{\theta} = \frac{1}{K_{ads}} + C_{inh} \tag{10}$$

where C_{inh} is the inhibitor concentration, θ is the fraction of surface covered, $\Delta G°_{ads}$ is the standard free energy of adsorption, R is the gases constant 8.314 J/mol.K, T is the temperature in Kelvin and K_{ads} is equilibrium constant of adsorption reaction and from intercept line on (concentration/θ) axis has been calculated as shown in Equation 11. Besides, standard free energy of adsorption has been calculated by the following Equation 12 [34,47,48].

$$\text{Intercept} = \frac{1}{K_{ads}} \tag{11}$$

$$\Delta G°_{ads} = -R \times T \times \ln(55.5\, K_{ads}) \tag{12}$$

Results of adsorption behavior have been listed in Table 5 and Figure 10. Infer that the plots of C_{inh}/θ versus C_{inh} produce the straight lines. Thus the average correlation coefficient 0.999990, 0.999991 and slopes 1.04848, 1.08855 have been calculated for both compounds **A1** and **A2**, respectively, indicating that the adsorption of compounds 3-(2-hydroxy-3-

methoxyphenyl)-5-(4-nitrophenyl)-2-(4-((4-nitrophenyl)diaz ennyl)phenyl)dihydro-2*H*-pyrrolo[3, 4-*d*]isoxazole-4, 6 (*5H, 6aH*)-dione and 5-(4-(1,3,5-dithiazinan-5-yl)phenyl)-5-pentyl-1,3,5-dithiazinan-5-ium have been subject Langmuir adsorption. The high values of the equilibrium constant of adsorption (K_{ads}) of compounds **A1** and **A2** are 5405.40 and 5586.59, respectively, reflecting the high capacity for adsorption these compounds on mild steel surface in cooling water. Thus the values of $\Delta G°_{ads}$ are negative -31.245 and -31.327 kJ/mol this suggests that a mixed type of adsorption has been occurred on surface which involves both physiosorption and chemisorption [38,47,49,50]. The negative values of $\Delta G°_{ads}$, which obtained, indicate to spontaneous adsorption of the inhibitors on the mild steel surface, and a low negativity refers to electrostatic interactions between inhibitor and the charged metal surface [51].

3.4. Quantum chemistry methodology

Recently, the density functional theory (DFT) has been used to analyze the properties of inhibitor and describe inhibition of metal surfaces; it is one of theoretical models used in explaining the chemistry and physics of solids. Furthermore, DFT is considered a very useful technique to analyse the experimental data, thus in the present investigation, the quantum chemical has been calculated by using density functional theory for explaining the experimental results obtained and to further give insight into the inhibitors action of compounds **A1** and **A2** on the mild steel surface [52,53]. On the other hand, the quantum chemical results show ability of molecular structure for donation and back donation between the molecule and the metal surface [3]. Quantum parameters of heterocyclic compounds included E_{HOMO}, E_{LUMO}, S, ΔE_{gap}, ΔN, ω, χ_{inh}, η_{inh}, μ and $\Delta E_{Back-donation}$. The number of transferred electrons (ΔN), denote the absolute electro negativity of inhibitor molecule (χ_{inh}) and the global hardness of the inhibitor molecule (η_{inh}) have been calculated by using Equations 13, 14 and 15, respectively [54-56].

$$\Delta N = \frac{\chi_{Fe} - \chi_{inh}}{[2(\eta_{Fe} + \eta_{inh})]} \quad (13)$$

$$\chi_{inh} = \frac{(I+A)}{2} \quad (14)$$

$$\eta_{inh} = \frac{(I-A)}{2} \quad (15)$$

According to Koopman's theorem, *I* is ionization potential which represents the (-E_{HOMO}), and *A* is electron affinity which represents the (-E_{LUMO}). The theoretical values used of χ_{Fe} and η_{Fe} are 7.0 and 0 eV/mol, respectively, according to Pearson's scale. The energy gap (ΔE_{gap}) has been calculated by using Equation 16, the inverse of the global hardness (η) designated as the global softness (*S*) as shown in Equation 17, the global electrophilicity index (ω) has been calculated by using Equation 18 [50,54-57].

$$\Delta E_{gap} = (E_{LUMO} - E_{HOMO}) \quad (16)$$

$$S = \frac{1}{\eta} = \frac{2}{E_H - E_L} \quad (17)$$

$$\omega = \frac{\chi^2}{2\eta} \quad (18)$$

The HOMO is the orbital that could act as an electrons donor since it is the outermost (highest energy), in other words it is orbital which contains electrons. The LUMO is the orbital that could act as the electron acceptor since it is the innermost (lowest energy), in other words it is orbital that has room to accept electrons. $\Delta E_{Back-donation}$ is directly proportional

to the hardness *(η)* of the molecule, and calculated as indicated in Equation 19 [3,54].

$$\Delta E_{Back-donation} = -\frac{\eta}{4} \quad (19)$$

The relation between the Fukui function *f (r)* and the local softness *S*(r) is given in Equation 20 [9,54].

$$S_{(r)} = \left(\frac{\partial \rho_{(r)}}{\partial N}\right) v_{(r)} \left(\frac{\partial N}{\partial \mu}\right) v_{(r)} = f_{(r)} S \quad (20)$$

From this relation it can be concluded that local softness *S(r)* is directly related with Fukui function *f (r)* closely, and it plays an important role in the field of chemical reactivity. The chemical reactivity of different sites of molecules is evaluated through Fukui indices. It is defined by for nucleophilic attack [9,54].

$$f k^+ = q_{N+1} - q_N \quad (21)$$

For electrophilic attack:

$$f k^- = q_N - q_{N-1} \quad (22)$$

where q_N, q_{N-1} and q_{N+1} are the electronic population of the atom *K* in neutral, cationic and anionic systems respectively. Ionization potential (*I*) has been calculated as indicated in Equation 23 [53,57].

$$I = -E_{HOMO} \quad (23)$$

The relationship between the E_{HOMO} and the inhibition efficiency can be represented by Equation 24 [6].

$$E_{HOMO} = 6.64 \times 10^{-4} \{\ln(eff\%) + 142.29\} \quad (24)$$

Figures 11 and 12 show that the relationship between E_{HOMO} values and inhibition efficiency is proportional relationship, the other words, increase of inhibition efficiency causes increase of E_{HOMO} values due to the increasing activation energy in presence of inhibitors as shown in Table 4. Also the positive values of E_{HOMO} indicate to the ability of inhibitors to adsorb on the mild steel, and the type adsorption is chemisorptions [1,3,6].
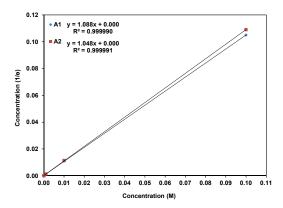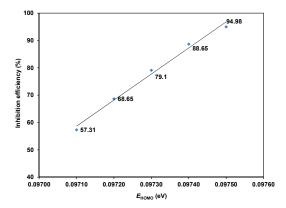

Figure 10. Langmuir isotherm adsorption of heterocyclic compounds **A1** and **A2** on the surface of mild steel in cooling water at 298 K.
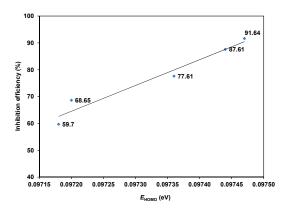
Frontier molecular orbital theory is useful and important in predicting adsorption centers of the inhibitor molecules responsible for the interaction with metal surface atoms. According to the molecular orbital theory of chemical reactivity, transitions of electron is due to interaction between highest occupied molecular orbital (HOMO) and lowest unoccupied molecular orbital (LUMO) for reactants [54,55].

Table 6. Quantum chemical parameters of studied compounds, calculated using B3LYP/6-31G (d,p).

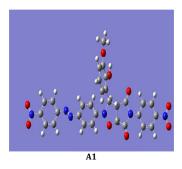| Quantum parameters	Compound A1	Compound A2
E_{HOMO} (eV)	-9.698	-5.0458
E_{LUMO} (eV)	-1.726	-1.6890
ΔE_{Gap} (eV)	7.972	3.3568
$\Delta E_{Back\text{-}donation}$ (eV)	-0.9965	-0.4196
Dipole moment μ (Debye)	-5.712	-3.3674
Transferred electrons ΔN	0.1615	1.0821
Electro negativity χ (eV/mol)	5.712	3.3674
Global hardness η (eV/mol)	3.986	1.6784
Global softness S (eV/mol)	0.2508	0.5958
Global electrophilicity ω	4.0926	3.3780
Ionization potential I (eV)	9.698	5.0458
Electron affinity A (eV)	1.726	1.6890
Chemical potential ɓ (eV)	-5.712	-3.3674

Figure 11. Relationship between E_{HOMO} and inhibition efficiency of compound **A1** at 298 K.

Figure 12. Relationship between E_{HOMO} and inhibition efficiency of compound **A2** at 298 K.

Heterocyclic compounds which have been studied differ in atoms number of carbon, nitrogen, oxygen and sulfur; also they differ in the number of aromatic rings. Figures 13-15 the optimized molecular structure and electronic distribution of HOMO and LUMO were showed, thus it was observed that these distributions were different, indicating the inhibition efficiency would be sensitive for it. For the compound **A1**, the HOMO density have been mainly concentrated on the nitrogen atoms, oxygen atom and benzene rings as shown in Figure 14, while LUMO it was distributed on the nitrogen atoms and oxygen atoms as well as on one benzene ring, thus unoccupied 3*d*-orbitals of Fe atoms can accept electrons from inhibitor molecule mainly using the nitrogen atoms, oxygen atom and benzene rings to form a coordinate bond, also the molecule of inhibitor can accept electrons from anti-bonding orbitals of Fe atoms to form back-donation bond. As for the compound **A2**, the HOMO density have been mainly concentrated on the benzene ring, while LUMO it was distributed on the nitrogen

atom and sulfur atoms, thus unoccupied 3*d*-orbitals of Fe atoms can accept electrons from inhibitor molecule using the electrons of benzene ring to form a coordinate bond, also the molecules of inhibitor can accept electrons from anti-bonding orbitals of Fe atoms to form back-donation bond. The high values of E_{HOMO} indicate a tendency of molecule to donate electrons to appropriate acceptor molecules with low energy. Similarly, the value of E_{LUMO} reflects the ability of the molecule to accept electrons. The low values of ΔE_{gap} imply that the good inhibition efficiency and they imply that the excitation energy to remove electron from the last orbital will be low. This indicates that the molecules of inhibitors **A1** and **A2** are more polarized with low in kinetic stability and will be termed as soft molecules or soft-soft interactions. Based on the results shown in Table 6, it was observed that the values of E_{LUMO} are low which indicates that the ability of inhibitor molecules on that accept electrons. Through looking at the distribution of LUMO in Figure 15 it was noted that molecule of **A1** inhibitor can easily accept electrons from the occupied 4s-orbital of Fe atoms by the benzene ring, oxygen atoms and nitrogen atoms to form binding forces between the inhibitor molecule and Fe atoms on the mild steel surface, while molecule of **A2** inhibitor can easily accept electrons of occupied 4s-orbital of Fe atoms by nitrogen atom and two sulfur atoms. Consequently this electronic acceptance could help to formation more stable bonds between inhibitor molecules and surface of mild steel [3,25,35,58-62].

According to the Lukovits's, if the value of the transferred electrons (ΔN) is less than 3.6, the inhibition efficiency increases through the increase of electron-donating ability of these inhibitors to the metal surface [54]. In this study it was observed that the values of ΔN are less than 3.6. They are 0.1615 and 1.0821 for compounds **A1** and **A2**, respectively, as shown in Table 6. This explains that inhibition efficiency has been increased with the increase of electron-donating ability. In another words, the ΔN values correlates strongly with experimental inhibition efficiency, hence the highest fraction of electrons transferred is associated with inhibitor which has the least efficiency (**A2**), while the least fraction of electrons transferred is associated with the inhibitor which has the best efficiency (**A1**) [3,54]. If the value of $\Delta E_{Back\text{-}donation}$ < 0 and value of global hardness η > 0, this implies that charge transfer to a molecule followed by a back-donation from the molecule, hence it is possible to compare the stabilization among inhibiting molecules, the interaction will be occurred with same metal, then global hardness decreases. At the meanwhile the results of this study were identical for it as shown in Table 6, if they were observed that the values of global hardness (η) are 3.986 and 1.6784 (η > 0) while the values of $\Delta E_{back\text{-}donation}$ are -0.9965 and -0.4196 (ΔE < 0) for compounds **A1** and **A2**, respectively. Fukui indices were used for the local reactivity description thus they can be only used for comparing atoms centers within the same molecule, also widely used to describe the selective site for soft-soft interaction, as well as, they were used for predicting the preferred site of electrophilic attack, whereas global softness allow the comparing between similar
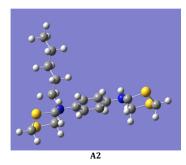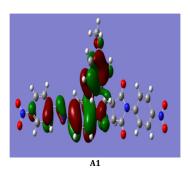
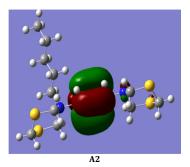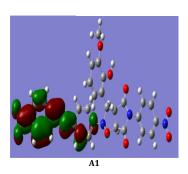**Figure 13.** Optimized molecular structures of compounds **A1** and **A2** by using B3LYP/6-31G (d,p).

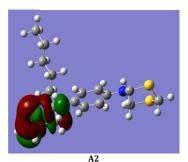**Figure 14.** The highest occupied molecular orbital (HOMO) density of compounds **A1** and **A2** using DFT at the B3LYP/6-31G(d,p).

Figure 15. The lowest unoccupied molecular orbital (LUMO) density of compounds **A1** and **A2** using DFT at the B3LYP/6-31G (d,p).

atoms for different molecules. Global electrophilicity index (ω) measures the stabilization of energy when the system acquires an additional number from transferred electrons (ΔN) which have been transferred from corrosion environment, therefore, it will be more reactive and a good nucleophile when its value low, and conversely will be a good electrophile when its value high, in this study it was observed that the value of (ω) are 4.0926 for compound **A1** and 3.3780 for compound **A2** [9,54]. Dipole moment was calculated according to the relationship (Dipole moment = - Electro negativity) [63]. The dipole moment (μ) is an index used for the prediction of the direction of a corrosion inhibition process, also it is the measure of polarity of covalent bond, and furthermore, it describes inhibitor polarity related in distribution of molecule electrons. The high value of dipole moment increases probably the adsorption processes among molecules of inhibitor and metal surface [1,3,55], it is generally agreed that adsorption of polar compounds possessing high dipole moments on the metal surface should lead to better inhibition efficiency [55]. In other literature, it was noted that low value of dipole moment (μ) will lead to the accumulation of inhibitor molecules on the metallic surface(adsorption occurs) [57], hence in this study it was noted that dipole moment values for compounds **A1** and

A2 are low as shown in Table 6, therefore it can conclude that compound **A1** has more inclination to the adsorb on the mild steel surface compared with compound **A2**, and finally the inhibition efficiency of compound **A1** is higher than compound **A2** and this underlines experimental results that the earlier reported.

4. Conclusions

The main conclusions drawn from this study are two compounds 3-(2-hydroxy-3-methoxy phenyl)-5-(4-nitro phenyl)-2-(4-((4-nitrophenyl)diazennyl)phenyl)dihydro-2*H*-pyrrolo[3,4-d]isoxazole-4,6(5*H*,6a*H*)-dione and 5-(4-(1,3,5-di thiazinan-5-yl)phenyl)-5-pentyl-1,3,5-dithiazinan-5-ium, possess high inhibition characteristics, indicating that they are excellent inhibitors for mild steel Q235 type in cooling water systems. Inhibition efficiency has been increased with increasing of concentration, and decreased with temperature raise for both compounds. The adsorption of inhibitor molecules subject to Langmuir adsorption isotherm. The positive values of ΔH° mean chemical adsorption was occurred, and the E_a values mean physical adsorption was occurred, therefore they infer that the mixed type of

adsorption has been occurred on the mild steel surface. Also, the negative values of $\Delta G°_{Ads}$ refer that the mixed type of adsorption was occurred. The positive values of enthalpy suggested that dissolution of mild steel in presence of inhibitors is slow. Quantum chemical calculations are on agreement with the experimental results, and show that the compounds **A1** and **A2** have the ability to electronic donation, thus they lead to strong adsorption on mild steel surface, in another words, theoretical results showed a good correlation confirming the reliability of the experimental results, and confirming on high inhibition efficiencies.

Acknowledgements

References

[1]. Loutfy, H. M.; Elroby, S. K. *Int. J. Ind. Chem.* **2015**, *6(3)*, 165-184.
[2]. Hikmat, A. R. A. *Engineering* **2017**, *9*, 254-262.
[3]. Al-Sabagh, A. M.; Notaila, M. N.; Ahmed, A. F.; Mohamed, A. M.; Abdelmonem, M. F. E.; Tahany, M. *Egypt. J. Petroleum* **2013**, *22*, 101-116.
[4]. Khaled, K. F.; Babic-Samardzija, K.; Hackerman, N. *Electrochim. Acta* **2005**, *50*, 2515-2520.
[5]. Altsybiera, A. I.; Levin, S. Z.; Dorokhov, A. P., Third European Symposium of Corrosion Inhibitors, University of Ferrara, Ferrara, Italy, 1971.
[6]. Al-Sawaad, H. Z. M. *J. Mater. Environ. Sci.* **2011**, *2(2)*, 128-147.
[7]. Granese, S. L. *Corros. Sci.* **1988**, *44*, 322-328.
[8]. Tadros, A. B.; Abdenaby, B. A. *J. Electro. Chem.* **1988**, *246*, 433-439.
[9]. Bincy, J.; Abraham, J. *Port. Electrochim. Acta* **2011**, *29(4)*, 253-271.
[10]. Bentiss, F.; Lagrenee, M. *J. Mater. Environ. Sci.* **2011**, *2(1)*, 13-17.
[11]. Elmsellem, H.; Karrouchi, K.; Aouniti, A.; Hammouti, B.; Radi, S.; Taoufik, J.; Ansar, M.; Dahmani, M.; Steli, H.; El Mahi, B. *Der Pharma Chemica* **2015**, *7(10)*, 237-245.
[12]. Zarrok, H.; Oudda, H.; Zarrouk, A.; Salghi, R.; Hammouti, B.; Bouachrine, M. *Der Pharma Chemica* **2011**, *3(6)*, 576-590.
[13]. Ehteram, A. N.; Aisha, H. *Mater. Chem. Phys.* **2008**, *110*, 145-154.
[14]. Riggs, O. L. J.; Hurd, R. M. *Corrosion* **1967**, *23*, 252-259.
[15]. Durnie, W.; Marco, R. D.; Jefferson, A.; Kinsella, B. *J. Electrochem. Soc.* **1999**, *146*, 1751-1757.
[16]. Guo-Hao, C.; Jing-Mao, Z. *Chem. Res. Chin. Univ.* **2012**, *28(4)*, 691-695.
[17]. Pavia, D. L.; Lampman, G. M.; Kriz, G. S. Introduction to Spectroscopy, 3rd edition, Thomson Learning Inc, USA, 2001.
[18]. Macomber, R. S., A Complete Introduction to Modern NMR Spectroscopy, John Wiley & Sons, Inc., Canada, 1998.
[19]. Pretsch, E.; Buhlmann, P.; Badertscher, M. Structure Determination of Organic Compounds, 4th Edition, Germany, 2009.
[20]. Noor, K. M. K.; Adibatul, H. F.; Karimah, K.; Shadatul, H. R.; Mohd, S. M. *Malays. J. Analy. Sci.* **2014**, *18(1)*, 21-27.
[21]. Saratha, R.; Vasudha, V. G. *J. Chem.* **2010**, *7(3)*, 677-684.
[22]. Gupta, N. K.; Quraishi, M. A.; Singh, P.; Srivastava, V.; Srivastava, K.; Verma, C.; Mukherjee, A. K. *Anal. Bioanal. Electrochem*. **2017**, *9(2)*, 245-265.
[23]. Nwabanne, J. T.; Okafor, V. N. *J. Emerging Trends Eng. Appl. Sci.* **2011**, *2(4)*, 619-625.
[24]. Ghazoui, A.; Saddik, R.; Benchat, N.; Guenbour, M.; Hammouti, B.; Al-Deyab, S. S.; Zarrouk, A. *Int. J. Electrochem. Sci.* **2012**, *7*, 7080-7097.
[25]. Obi-Egbedi, N. O.; Obot, I. B. *Arab. J. Chem.* **2013**, *6*, 211-223.
[26]. Xiang-Hong, L.; Xiao-Guang, X. *Acta Phys. Chim. Sin.* **2013***, 29(10)*, 2221-2231.
[27]. Awe, F. E.; Idris, S. O.; Abdulwahab, M.; Oguzie, E. E. *Mater. Chem.* **2015**, *1*, 111-118.
[28]. Ayssar, N.; Abu-Abdoun, I.; Abdel-Rahman, I.; Al-Khayat, M. *Int. J. Corros.* **2010**, ID: 460154, 1-9.
[29]. Yadav, M. ; Kumar, S. ; Purkait, T. ; Olasunkanmi, L. O. ; Bahadur, I.; Ebenso, E. E. *J. Mol. Liq.* **2016**, *213*, 122-138.
[30]. Amin, M. A.; Abd El-Rehim, S. S.; El-Sherbini, E. E. F.; Bayoumi, R. S. *Int. J. Electrochem. Sci.* **2008**, *3*, 199-215.
[31]. Al-Juaid, S. S. *J. Port. Electrochim. Acta* **2007**, *25*, 363-373.
[32]. El-Khattabi, O.; Zerga, B.; Sfaira, M.; Taleb, M.; Ebn Touhami, M.; Hammouti, B.; Herrag, L.; Mcharfi, M. *Der Pharma Chemica* **2012***, 4(4)*, 1759-1768.

[33]. Sudhish, K. S.; Ashish, K. S.; Quraishi, M. A. *Int. J. Electrochem. Sci.* **2011**, *6*, 5779-5791.
[34]. Ashish, K. S.; Quraishi, M. A. *Int. J. Electrochem. Sci.* **2012**, *7*, 3222-3241.
[35]. Pournazari, S.; Moayed, M. H.; Rahimizadeh, M. *J. Corros. Sci.* **2013**, *71*, 20-31.
[36]. Eddy, N. O.; Odoemelam, S. A.; Odiongenyi, A. O. *Adv. Natural Appl. Sci.* **2008**, *2(1)*, 35-42.
[37]. Szyprowski, A. J. *J. Corros.* **2003**, *59(1)*, 68-81.
[38]. Mobin, M.; Masroor, S. *Int. J. Electrochem. Sci.* **2012**, *7*, 6920-6940.
[39]. Dahmani, M.; Et-Touhami, A.; Al-Deyab, S. S.; Hammouti, B.; Bouyanzer, A. *Int. J. Electrochem. Sci.* **2010**, *5*, 1060-1069.
[40]. Fouda, A. S.; Al-Sarawy, A. A.; El-Katori, E. E. *Desalination* **2006**, *201*, 1-13.
[41]. Boukalah, M.; Hammouti, B.; Lagrenee, M.; Bentiss, F. *Corros. Sci.* **2006**, *48*, 2831-2837.
[42]. Khadom, A. A.; Yaro, A. S.; Aitaie, A. S.; Kadum, A. A. H. *Port. Electrochim. Acta* **2009**, *27(6)*, 699-712.
[43]. Ebenso, E. E.; Alemu, H.; Umoren, S. A.; Obot, I. B. *Int. J. Electrochem. Sci.* **2008**, *3*, 1325-1339.
[44]. Guan, N.; Xueming, L.; Fei, L. *Mater. Chem. Phys.* **2004**, *86*, 59-68.
[45]. Muthukrishnan, P.; Jeyaprabha, B.; Prakash, P. *Int. J. Indus. Chem.* **2014**, *5(4)*, 1-11.
[46]. Saratha, R.; Priya, S. V.; Thilagavathy, P. *Eur. J. Chem.* **2009**, *6(3)*, 785-789.
[47]. Fouda, A. S.; Elewady, G. Y.; Shalabi, K.; Habbouba, S. *J. Mater. Environ. Sci.* **2014**, *5(3)*, 767-778.
[48]. Lahmidi, S.; Elyoussfi, A.; Dafali, A.; Elmsellem, H.; Sebbar, N. K.; El Ouasif, L.; Jilalat, A. E.; El-Mahi, B.; Essassi, E. M.; Abdel-Rahman, I.; Hammouti, B. *J. Mater. Environ. Sci.* **2017**, *8 (1)*, 225-237.
[49]. Lutendo, C. M.; Mwadham, M. K.; Eno, E. E. *J. Mol. Liq.* **2016**, *215*, 763-779.
[50]. Adardour, L.; Lgaz, H.; Salghi, R.; Larouj, M.; Jodeh, S.; Zougagh, M.; Hamed, O.; Taleb, M. *Der Pharm. Lett.* **2016**, *8 (4)*, 173-185.
[51]. Adejoro, I. A; Ibeji, C. U; Akintayo, D. C. *Chem. Sci.* **2017**, *8(1)*, 1-6.
[52]. Junaedi, S.; Al-Amiery, A. A.; Kadihum, A.; Kadhum, A. H.; Mohamad, Abu Bakar *Int. J. Mol. Sci.* **2013**, *14*, 11915-11928.
[53]. Elazhary, I.; Ben, H.; Laamari, M. R.; El- Haddad, M.; Rafqah, S.; Anane, H.; Moubtassim, M. L. E.; Stiriba, S. E. *J. Mater. Environ. Sci.* **2016**, *7(4)*, 1252-1266.
[54]. Udhayakalaa, P.; Rajendiranb, T. V.; Gunasekaranc, S. *J. Adv. Sci. Res.* **2012**, *3(2)*, 71-77.
[55]. Raja, K.; Senthilkumar, A. N.; Tharini, K. *Adv in Appl. Sci. Res.* **2016**, *7(2)*, 150-154.
[56]. Nirmala, B.; Manjula, P. *Int. J. Inno. Sci. Res.* **2016**, *5(3)*, 3977-3985.
[57]. Paulin, M. N.; Drissa, S.; Albert, T.; Assemian, Y.; Henri, K. A.; Donourou, D. *J. Soc. Ouest-Afr. Chim.* **2010**, *30*, 49-58.
[58]. John, S.; Joseph, A. *Mater. Chem. Phys.* **2012**, *133*, 1083-1089.
[59]. Junaedi, S.; Kadhum, A. H.; Al-Amiery, A. A.; Mohamad, A.; Takriff, M. S. *Int. J. Electrochem. Sci.* **2012**, *7*, 3543-3554.
[60]. Nnenna, W. O.; Jonathan, O. B.; Ekemini, B. I.; Abiodun, O. E. *American J. Phys. Chem.* **2015**, *4*, 1-9.
[61]. Cherrak, K.; Dafali, A.; Elyoussfi, A.; El Ouadi, Y.; Sebba, N. K; El Azzouzi, M.; Elmsellem, H.; Essassi, E. M.; Zarrouk, A. *J. ater. Environ. Sci.* **2017**, *8(2)*, 636-647.
[62]. Qian, Z.; Tiantian, T.; Peilin, D.; Zhiyi, Z.; Fang, W. *Metals* **2017**, *7(44)*, 1-11.
[63]. Nithya, P.; Rameshkumar, S.; Sankar, A. *Chem. Sci. Rev. Lett.* **2017**, *6(21)*, 20-30.